FARADAY ROTATION OF JUPITER'S DECAMETRIC RADIATION

M. Y. Boudjada*, G.A. Dulk†, and A. Lecacheux*

Abstract

We report on observations of Jovian decametric emission (DAM) obtained with the array of 144 log–periodic antennas at Nançay (France) coupled to a wide band (10–40 MHz) sweep frequency polarimeter. We show, from the study of Faraday effect on Jovian emission, that the linear approximation where the total rotation is proportional to the inverse frequency squared (ν^{-2}) is not sufficient to explain the observations. Then we use the quadratic approximation which is better able to explain the observations because it includes the difference between the X and O mode ray paths and the high density gradients of the ionosphere. We find for three Io–B emissions that the polarization ellipse at Jupiter appears to be roughly aligned with the Jovian rotation axis, unlike five Io–A events which exhibit really a random distribution.

1 Introduction

All the planetary auroral emissions are all strongly polarized. The study of this polarization is important because it can put strong constraints on the emission mechanism and on the propagation of the waves in the plasma surrounding the source.

The Jovian decametric radiation (DAM) is the only one which can be observed from the ground. The early observations revealed that it is strongly circularly polarized, but an important amount of linear polarization has also been observed [Warwick and Dulk, 1964; Parker et al., 1969; Lecacheux, 1976]. Two characteristics of the linear polarization are particularly interesting: First, the degree of linear polarization (or the ellipticity of the polarization ellipse) and its change with time, from one source to another, with the geometry of observations, etc., and second, the position angle of the linear component.

*CNRS–URA 324 and D.A.S.O.P., Observatoire de Paris, 92195 Meudon, France
†Depart. Astrophys., Planet. and Atmos. Sciences, University of Colorado, Boulder, CO 80309, USA

1.1 Linear approximation

When a linearly polarized wave enters an anisotropic plasma, it splits into the two characteristic magnetoionic modes, the ordinary (o) and extraordinary (x) waves. Each wave has its own polarization, depending on the orientation of the ambient magnetic field. Both modes propagate independently and the polarization of the propagating wave can be deduced from the polarization changes of both modes by adding in phase their electric fields. It can be shown [Budden, 1985] that the polarization change is simply a rotation Ω of the polarization plane due to the phase velocity difference of the two modes as they propagate

$$\Omega \,=\, \frac{1}{2}\,\Delta\,\phi$$

$$\text{with}\;\; \Delta\,\phi \,=\, \phi_o \,-\, \phi_x \,=\, \frac{2\,.\,\pi\,.\,\nu}{c}\,\{\int_{o\,ray\,path} n_o\,ds \,-\, \int_{x\,ray\,path} n_x\,ds\,\}\;, \qquad (1.1)$$

where ν is the wave frequency, c the light velocity, n_o and n_x the real parts of the refractive indices for the two modes, and ds an elementary ray path.

If we describe the ionosphere as a plasma slab, with uniform density and constant magnetic field, we obtain the well known formula

$$\Omega \,=\, \frac{\pi\,.\,\nu}{c}\,\int_{ray\,path}[\,n_o \,-\, n_x\,]\,ds \,=\, C_0^1 \,+\, \frac{C_1^1}{\nu^2}\;, \qquad (1.2)$$

where the integral is taken along the same paths for the (o)– and (x)–modes between the source and the radiotelescope. The Faraday rotation is thus a linear function of the inverse square of the frequency. The two constants C_0^1 and C_1^1 have to be measured. C_0^1 is the polarization angle at Jupiter, with an uncertainty of $\pm\,n\pi$. C_1^1 is proportional to the ionospheric electron content along the ray path

$$C_1^1 \,\propto\, \int_{ray\,path} B\,N_e\,\cos\theta\,ds \;\approx\; \langle\,B_{\parallel}\,\rangle\,.\,\langle\,N_e\,\rangle\,.\,L\;, \qquad (1.3)$$

where B is the magnetic field intensity, N_e the electron density, θ the wave normal angle and L is the path length ($<>$ mean spatial average).

The determination of the amount of Faraday rotation between the source and the observer is needed to deduce the position angle of the linear component of the emitted wave at the source from the measured position angle of the linear component at the Earth.

1.2 Effect of terrestrial Faraday rotation

There have already been several studies of the Faraday rotation of the linear component of the Jovian decametric emission; they all use the variation of the intensity with frequency (Faraday fringes) when Jupiter is observed with a linearly polarized antenna. Warwick and Dulk [1964] first showed that at least 90% of the rotation come from the Earth's ionosphere, only at most 10% being due to the Jovian magnetosphere. However, on a sample of 8 storms, Straka et al. [1965], comparing with ionospheric sounding experiments,

found more Faraday rotation in the spectra than could be accounted for by the terresterial ionosphere, and Riihima [1967] confirmed this result. At the same time Parker et al. [1969] extending the work of Warwick and Dulk, were able to determine the polarization angle at Jupiter. In a recent study, Phillips et al. [1989] stated that an appreciable fraction of the observed Faraday rotation, up to 30%, might occur in the Jovian magnetosphere. From the University of Florida observations they reported the detection of Faraday rotation in the vicinity of Jupiter for six Io–B storms. A single Io–A was analysed, and it exhibited no more Faraday rotation than that due to Earth's ionosphere. However, Lecacheux [1976], also studying the Faraday fringes on Jovian dynamic spectra, suggested that the approximations used in the analyses, referred to above, that the rotation Ω at the frequency ν is proportional to ν^{-2}, is not sufficiently accurate to allow a proper determination of the polarization angle at the source, and that higher order approximations must be used.

In this paper we present new observations obtained with a spectropolarimeter operated at Nançay since 1986. This instrument is able to provide the instantaneous Stokes parameters in a large range of frequencies (10–40 MHz). It is used as a synoptic instrument for about 6 hours a day, so many Jovian storms have been observed. The present work gives the first accurate measurements of the angle of polarization ellipse at Jupiter.

2 Equipment

The array at Nançay (France) consists of two arrays, one receiving right–hand circular (RHC) radiation and the other left–hand circular (LHC) radiation [Boischot et al., 1980]. Each array consists of 72 conical helix antennas [Erickson and Fisher, 1974] with a gain of 25 dB. The array is controlled by computer to track a source for about $\pm$ 3 hours centered on meridian transit.

The amplified outputs, V_1 and V_2 of the two arrays (Figure 1), are sent to the spectropolarimeter which adds them in phase and in phase–quadrature, correlates them, and provides four outputs from which the four Stokes parameters I, Q, U and V are deduced. The spectropolarimeter characteristics for the observations are the following: the frequency coverage was 10 to 40 MHz, swept in 1.2 or 2.5 seconds, with a frequency spacing of 250 or 125 kHz, a bandwidth of 30 kHz, a time constant of 10 ms, a duty cycle of 5 ms, and a number of frequency channels per sweep of 120 or 250.

3 Measure of the angle of polarization ellipse at Jupiter

3.1 Example of spectropolarimeter dynamic spectrum

Figure 2 shows the observed Stokes parameters, I and Q, as a function of frequency and time during a representative Io–B storm. Figure 2a displays a grey scale plot of the logarithm of the flux density as a function of time and frequency. There are 95 frequency channels, from 15.75 to 39.25 MHz. The time range covers 128 minutes, with the value at each minute being the average of 5 samples. Vertical lines due to calibration sequences

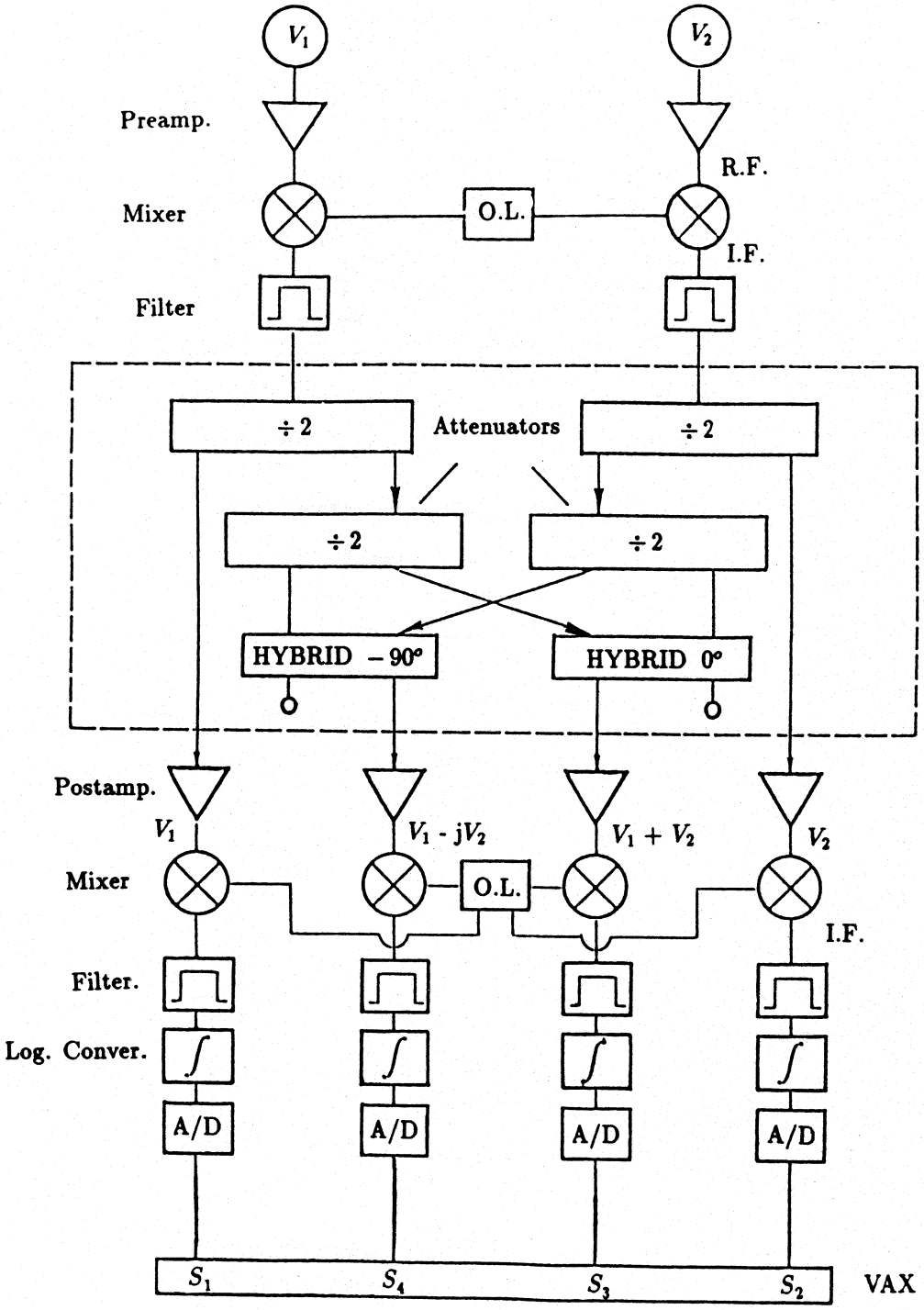

Figure 1: Block diagram of the spectropolarimeter. The two inputs V_1 and V_2 are connected to right and left circular arrays. The four outputs (the total right and left intensities, and the product of the polarized components RL and LR) are proportional to the L and R circular, and Q and U linear polarization event (R.F. = radio frequency, I.F. = intermediate frequency).

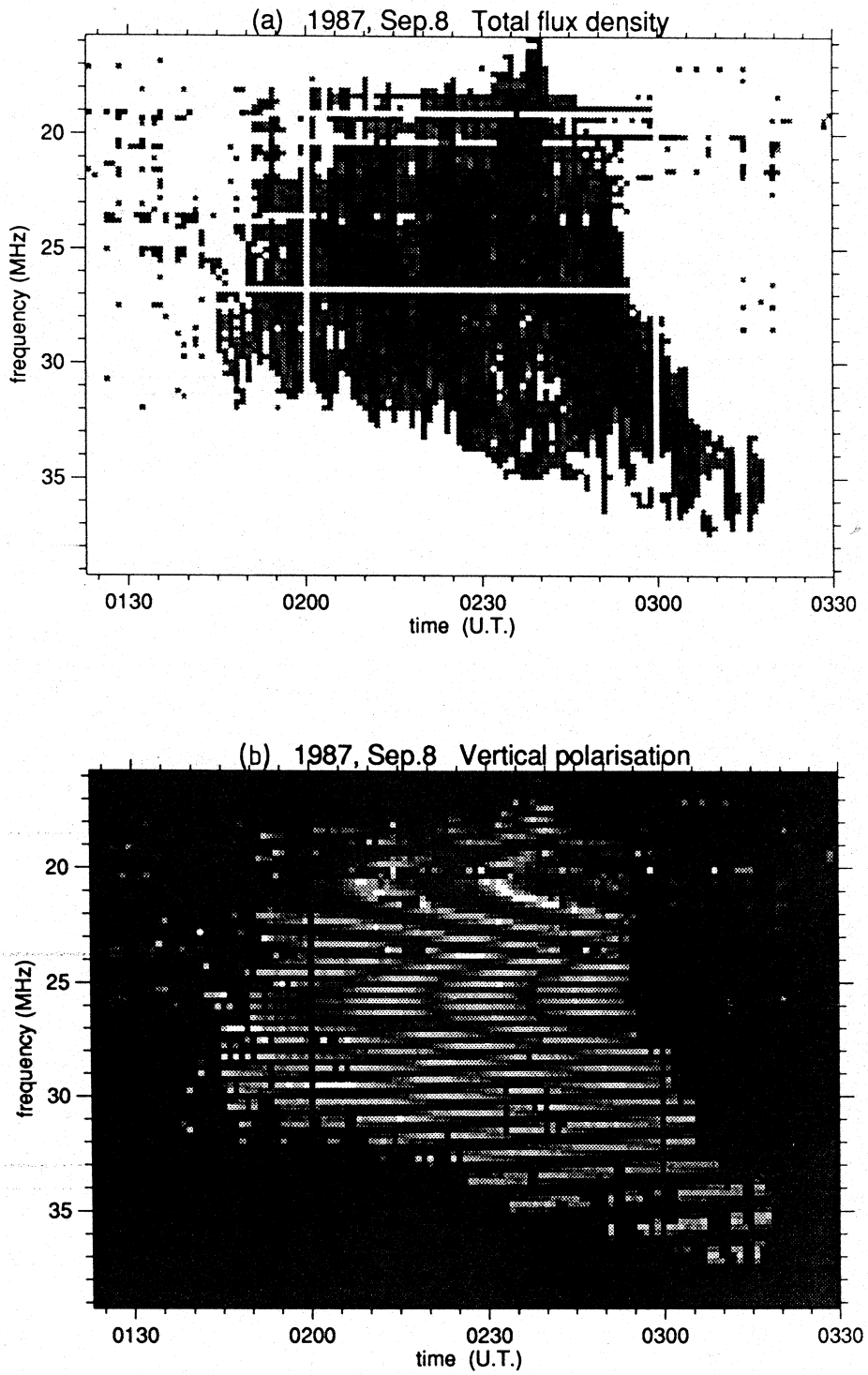

Figure 2: Dynamic spectra of the Io–B event on Sep. 8, 1987. (a) Total flux density (I): The darkness of the grey shading is proportional to signal intensity. (b) Linear polarization parameter (Q): The Faraday fringes appear as a nearly horizontal modulation of the Jupiter emissions. The fringes are widely spaced at high frequencies, and narrowly spaced at low frequencies. Below 22 MHz the curved fringes are due to the beating between the Faraday fringes and the sampling in frequency and time.

are noticeable at 0200 and 0300 U.T. The curved arc pattern at low frequencies is due to the beating between the frequency sampling and the Faraday fringe spacing.

Figure 2b shows the dynamic spectra of the linear Stokes parameters Q, corresponding to the vertical synthesized linear antenna which would have the same aperture as the original circularly polarized arrays. Alternating black and white fringes are due to Faraday rotation, corresponding to frequencies where the arriving signal antenna polarization was N–S (black) and E–W (white), respectively. The Farady fringes appear as a nearly horizontal modulation of the Jupiter emission. The fringes are widely spaced at high frequencies, and narrowly spaced at low frequencies.

3.2 Method of analysis

From the precedent spectropolarimeter dynamic spectrum, we select spectra obtained at successive times which were individually studied. From the individual values of Q and U, we can describe the apparent wave ellipse orientation by the angle $\chi = 0.5 \times \tan^{-1}(\mathrm{U/Q})$; the variations between $-90°$ and $90°$ are displayed in Figure 3. Note that about 22 half rotations of the ellipse are well measurable, with an average of 3 measurements per half rotation. The fringe spacing is larger at higher frequencies ($\approx$ 35 MHz) and decreases towards lower frequencies ($\approx$ 22 MHz), as expected.

Let $\{\nu_i\,,\,\chi_i\}_{i=1,N}$ be the measurement set, where at frequency ν_i, we have

$$\Omega(\,\nu_i) \;=\; \chi_i \;+\; k_i\,\pi\;. \tag{3.1}$$

We can arbitrarily number the measured half–rotations by taking $k_i = 0$ at the highest frequency. We find that the determination of k_i by visual inspection of the dynamic

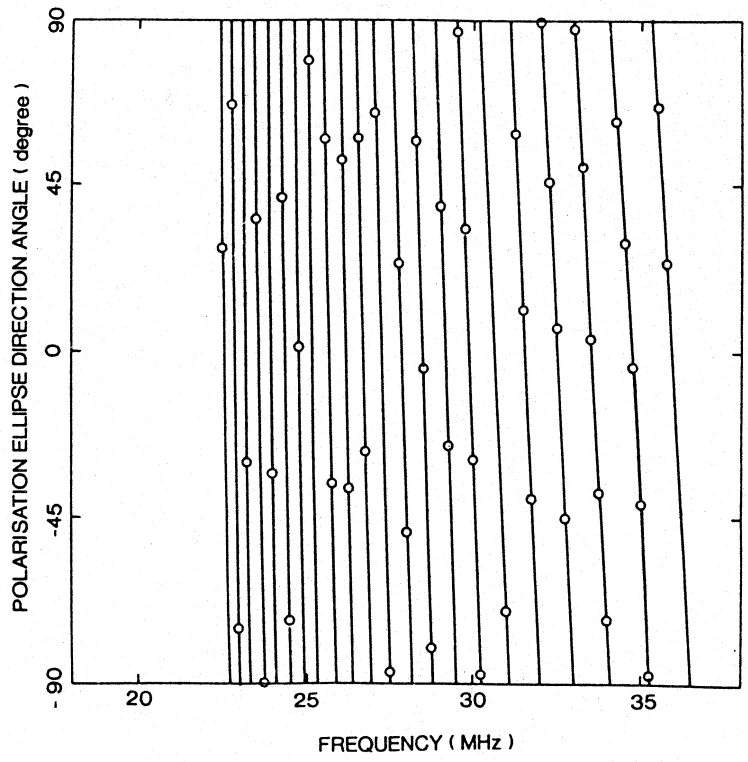

Figure 3: Example of the computed polarization as a function of frequency at a given time (0230 UT) for the Io–B storm Sep. 8, 1987. Angle of polarization ellipse shows widely–spaced fringes at high frequencies and closely–spaced at low frequencies.

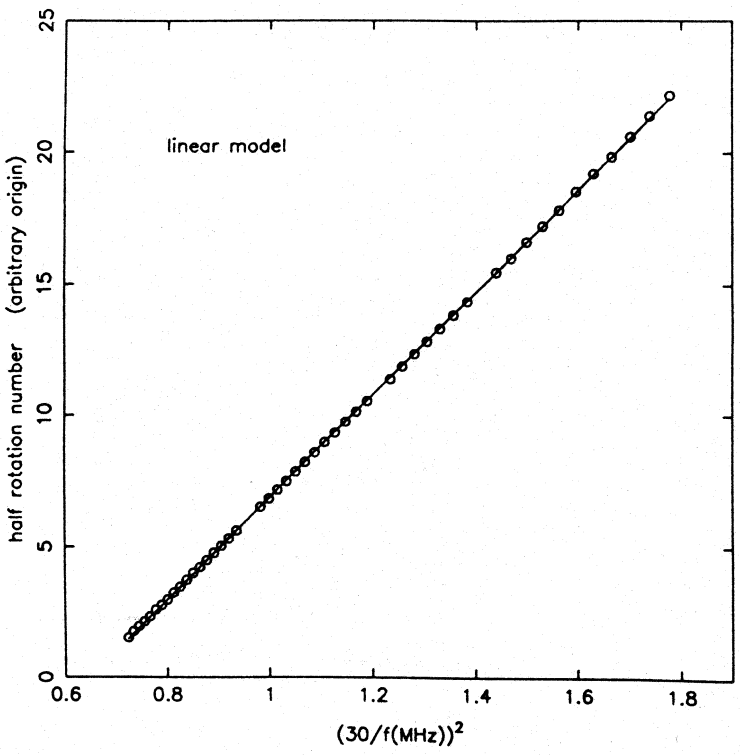

Figure 4: (a) Fit of the linear model from data of 0230 *UT, Sep. 8,* 1987*, as a function of inverse frequency squared.*

spectra is easy and not ambigous. So, from Equation 1.2, we have the following set of equations

$$\left\{ C_0^1 + \frac{C_1^1}{\nu_i^2} = \chi_i + k_i \pi \right\}_{i=1,N} . \tag{3.2}$$

For clarity, in the following, we will replace the unknown constant C_0^1 by C_0^1/π and C_1^1 by $C_1^1/[\pi(30)^2]$, so that we will measure the frequency in units of 30 MHz, and the angles in units of π.

The C_0^1 and C_1^1 constants are obtained from Equation 3.2 by fitting a straight line using the least squares method. The result is displayed in Figure 4a. At first sight, the fit appears to be very good throughout the whole frequency interval of more than one octave. But Figure 4b shows that the residuals from this linear fit are not randomly distributed and that they are clearly a function of frequency.

So Equation 1.2 does not adequately describe the observations, as was noticed by Lecacheux [1976]. Faraday rotation in the ionosphere is not as simple as assumed in Section 1, and the refraction of the waves at decameter wavelength cannot be neglected. The non–uniform distribution of the ionization as a function of altitude causes the O– and X–rays to be refracted along different, curved ray paths. Since the medium is anisotropic, the wave normal and the ray for a given characteristic mode are not coincident in direction. Full ray tracing, using a representative ionospheric model, is thus required to accurately compute the amount of Faraday rotation suffered by the decameter waves from Jupiter. Ross [1965] has shown that the non–uniformity of the electron density and the refraction of the rays can be taken into account with high accuracy by simply adding a third term

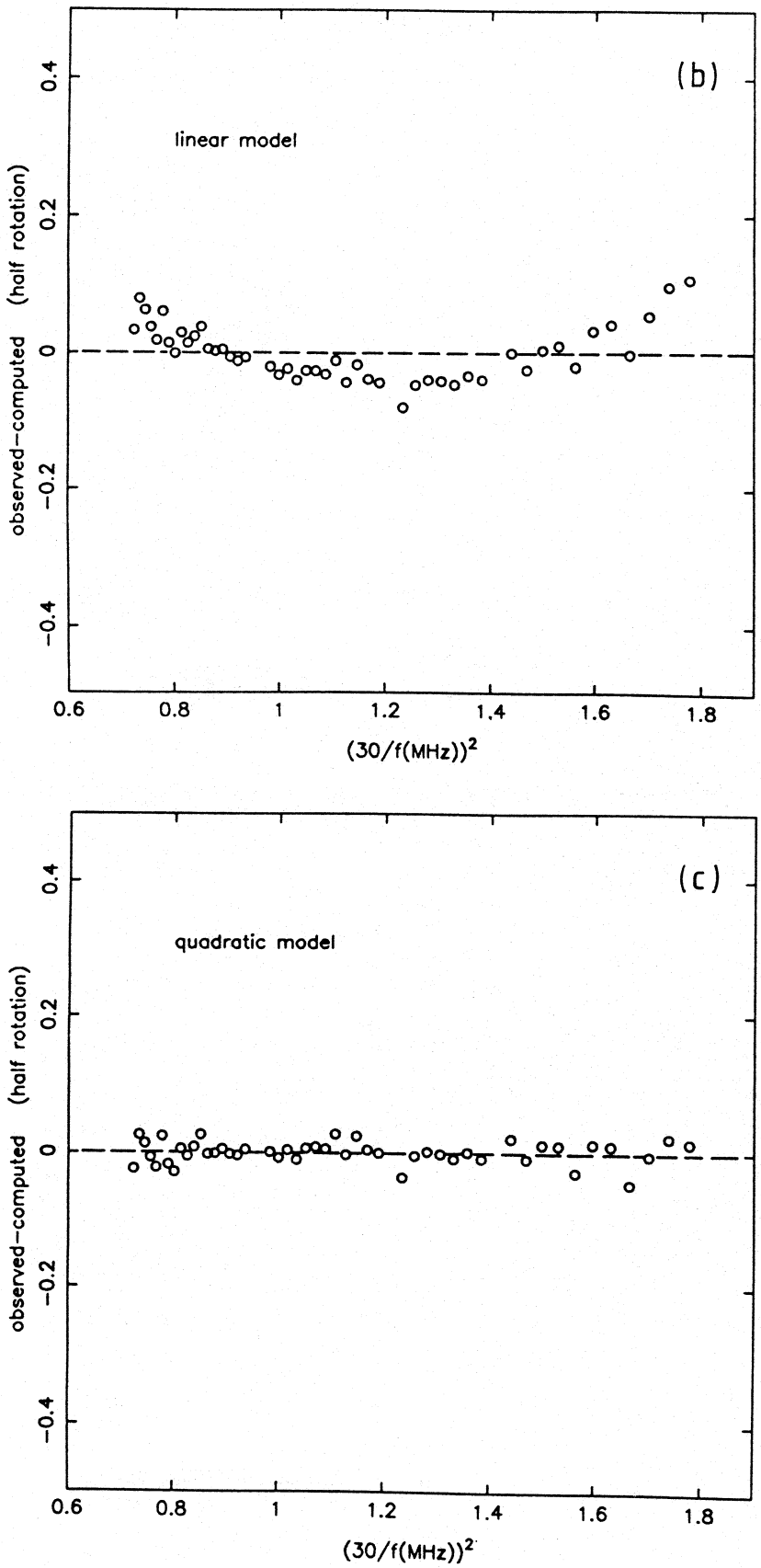

Figure 4: (b) Residuals (linear model). (c) Residuals (quadratic model).

in ν^{-4} to Equation 1.2, leading to

$$\Omega = C_0^2 + \frac{C_1^2}{\nu^2} + \frac{C_2^2}{\nu^4} \ . \tag{3.3}$$

Here C_0^2 still is the polarization angle to a factor of π, and C_1^2 and C_2^2 are measurements of rotation measure which depend on the plasma parameters and geometric properties of the ionosphere and the line of sight.

By using orthogonal Chebyshev polynominals, it is possible to fit the formula 3.3 with the Equation 3.2. Comparison of the fit using the linear formula 1.2 or by adding higher–order terms (ν^{-6}, etc...) is also very easy. Numerical simulations and computations for a number of cases (see below) show that the measurement accuracy allows us, in general, to retain the quadratic term, and so to obtain a better estimate of the position angle at Jupiter. For example, Figure 4c depicts the behaviour of the residuals after the fit of formula 3.3 with the data of Figure 3. They now appear to be randomly distributed. The value of C_0 determined from Equation 3.3 is different from that using Equation 3.2 by more than half a rotation. These observations agree with expectations, showing that Equation 3.3 is a reasonable description of the phenomenon.

For every analysed storm we used this method where we perform several cuts at intervals of a few minutes within each event. Spurious interferences were eliminated and the sky background was determined interactively by using a graphic workstation. A quadratic fit (Equation 3.3) was systematically computed, leading to the simultaneous determination of the position angle C_0^2 and the rotation measure C_1^1 and C_2^2, in the linear and quadratic approximations.

4 Statistical results

We present here the results of our analysis of eleven Jovian decameter storms recorded at Nançay between Oct. 1986 and Jan. 1989. They mainly correspond to Io–controlled emissions with high signal to noise ratios. We selected five Io–A and six Io–B storms. Figure 5 displays the CML–Io–phase diagram for our observations and Table 1 gives the list of all events with their characteristics.

The starting and ending times of polarization measurements are given, followed by the characteristic number of measured fringes (i.e half rotations of the polarization plane), the number of spectral cuts measured in each event. The maximum measured frequency is also given, together with the average and the standard deviation of the polarization angle, assumed to be a constant throughout the entire storm. Geometrical corrections were performed so that the angle given in the table is that measured from Jupiter's north pole, from north to east. We note that the frequency range of the measured Faraday data extends from 22 MHz to 33–36 MHz for all Io–B events. In the case of Io–A events, the highest frequency exceeds 29 MHz in only one case.

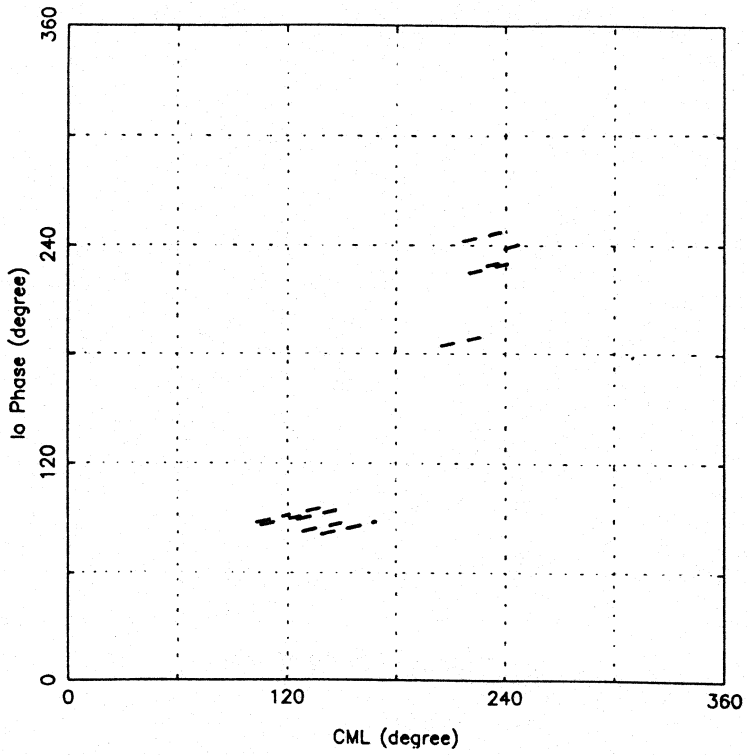

Figure 5: Locations of the Faraday events as a function of CML and Io–phase.

Table 1: List of analysed events with their characteristics.

Date	Time 1	Time 2	Fringes	Nb of data pt	Spectrum numbers	f (MHz)	Ω	σ	Source
October 20,86	21:20	21:50	25	284	7	34	+21.6	22.0	B
November 21,86	18:22	18:45	19	227	6	35	+30.0	22.3	B
December 23,86	14:35	15:15	43	650	9	35	-17.0	36.0	B
September 8,87	02:10	02:55	19	436	10	36	+12.5	7.8	B
September 15,87	03:30	04:05	18	336	9	33	+4.4	51.0	B
November 5,87	22:01	22:40	23	518	9	28	+15.8	43.0	A'
November 12,88	21:35	22:25	35	754	11	32	-4.0	42.0	B
December 4,88	21:40	22:15	17	534	8	34	-31.1	8.4	A
December 11,88	23:00	23:25	25	338	6	29	-17.2	55.0	A
December 18,88	23:10	23:50	37	536	7	29	-22.5	53.0	A
January 19,89	19:40	19:55	30	223	4	29	+30.0	50.0	A

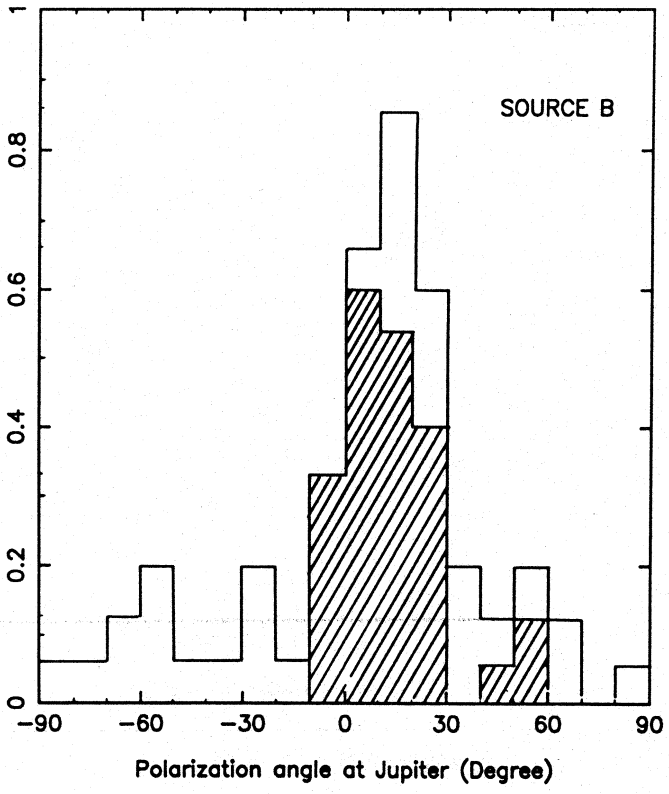

Figure 6: Results of the statistical analysis of the polarization angle at Jupiter. The unshaded histogram includes all the Io–B storms, and only those close to meridian transit are included in the shaded histogram.

4.1 Io–B storms

Figure 6 shows the histogram of the measured values of mod(C_0,π) for all spectral cuts in the Io–B events of Table 1. The distribution shows a well–peaked maximum, with a mean value of 7° and standard deviation of 34°. Looking more carefully, the distribution is made of a peak surrounded by a plateau, the latter corresponding to random occurrence of polarization angles anywhere between -90 and +90 degree; this plateau corresponds to measurements made two or more hours from the meridian.

Three events occur less than 1 hour from meridian transit, with roughly the same electron content. On the contrary, the computed contribution of the Earth's ionosphere is much more variable if we consider the events occurring ± 2 hours or more from the meridian. We conclude that, the larger the amount of Faraday rotation, the more inaccurate is the determination of C_0. This result leads us to disregard the events measured far from the meridian transit time; the resulting histogram is the hatched region displayed in Figure 6. So for most accurate measurements done during 3 Io–B events the mean value is +15° and the standard deviation is 13°. Thus the linear component of the polarization ellipse appears to be nearly aligned with the Jovian rotation axis.

4.2 Io–A storms

For source A events, the measurements of C_0^2 are displayed in Figure 7. The measured values are widely scattered and appear to be unreliable, in spite of all corrections.

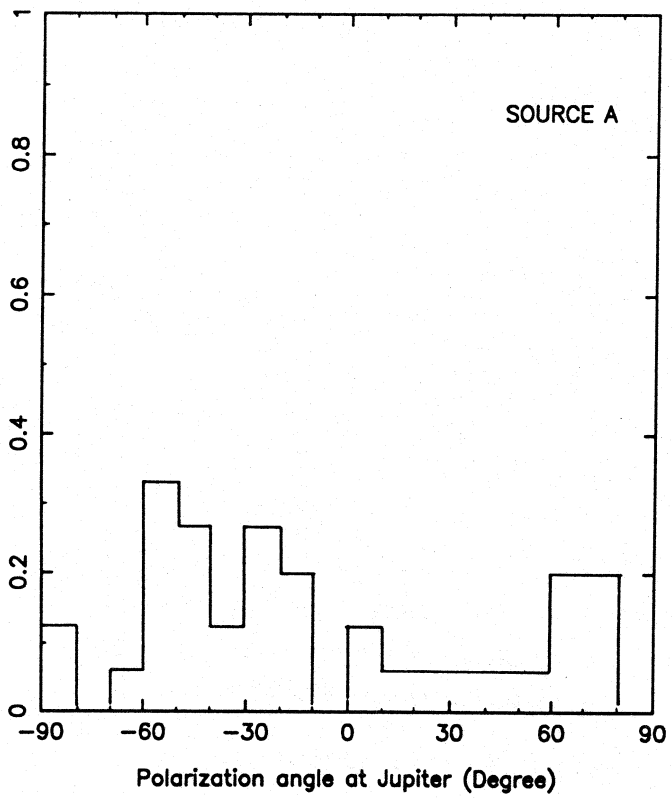

Figure 7: Results of the analysis of the polarization angle at Jupiter for the Io–A storms.

5 Discussion

Regarding the measure of the orientation of the linear component we find a difference between Io–A and Io–B storms. We suggest three reasons to explain why these results differ from the consistent ones as found for source B.

First, the usable frequency range is narrower for source A than for source B and occurs at lower frequencies (namely 22–29 MHz instead of 22–34 MHz). The depolarization due to the bandwidth (30 kHz), and the narrow fringe spacing at lower frequencies prevents high accuracy.

Second, the observed Io–A storms were not as intense as those of Io–B. This leads to a lower signal to noise ratio, and the uncertainty in the background level determination becomes more important.

Third, from the histogram in Figure 8, which shows the distribution of linear and circular polarization degrees in both source emissions, it appears that Io–A events have a lower degree of linear polarization than the Io–B events. Lecacheux and al. [1991] report on the complete Stokes polarimetry, as a function of both frequency and time, of two Io–related radio bursts (Io–B event: Sept. 15, 1987; Io–A event: Dec. 4, 1988) which we use in our investigation. They show that for: (a) Io–B event the radiation is primarily linear, with the degree of linear polarization averaging $\langle P_l \rangle \simeq 0.85$ and the degree of circular polarisation $\langle V/I \rangle \simeq -0.52$; (b) Io–A event the radiation is rather more circular, with $\langle P_l \rangle \simeq 0.66$ and $\langle V/I \rangle \simeq -0.76$. This measure confirms that Io–A events have a lower

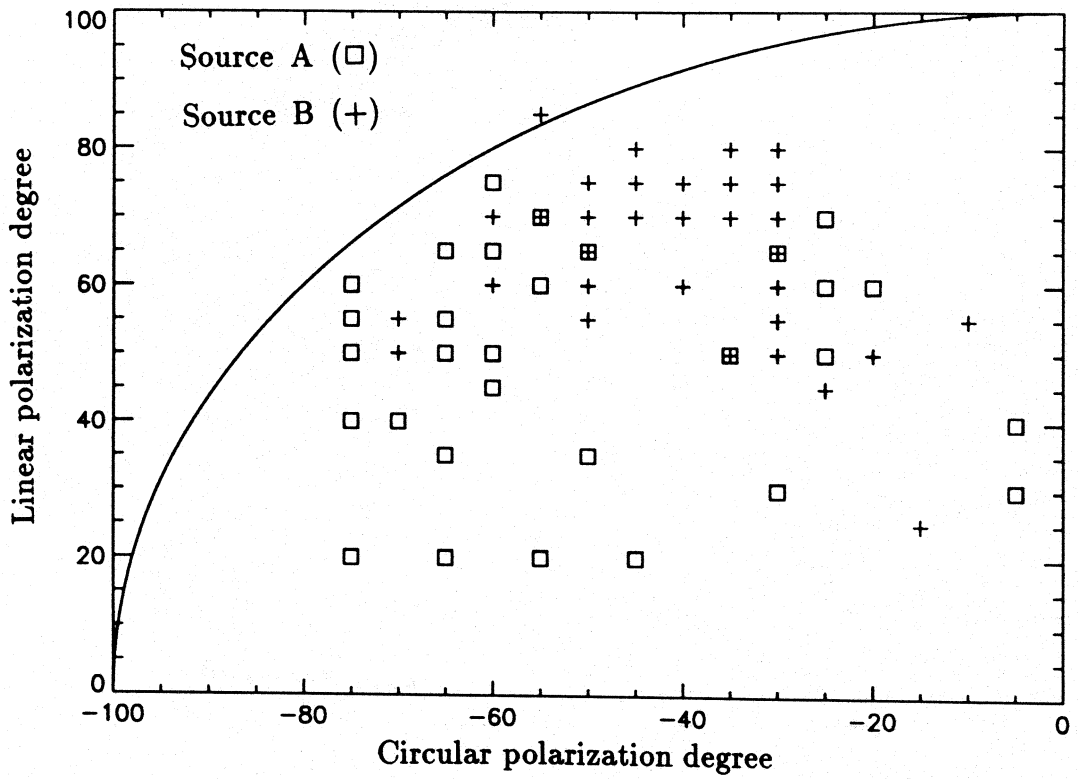

Figure 8: Distribution of the circular and linear polarization all for the Io–A and Io–B events.

degree of linear polarization than Io–B events.

Parker et al. [1969] were the only previous authors who tried to determine the orientation of the polarization ellipse at Jupiter. Using a linear approximation which probably under–estimated the position angle by up to π radians, they found an average position angle of $-25° \pm 15°$ with respect to the magnetic dipole. In addition, their spectral resolution (600 kHz) was not good enough to allow measurements of a large number of fringes. Compared with Parker et al. (Table 1 of their paper), we were able to utilize two to three times more Faraday fringes because of our better spectrograph resolution (30 kHz).

We have obtained reliable and consistent measurements of the polarization angle at Jupiter for six Io–B storms. All of them display a nearly constant and identical direction for the major axis of the polarization ellipse, which appears to be roughly aligned with the Jovian rotation axis. The geometry is depicted in Figure 9 for the best example of an Io–B and an Io–A event, assuming that the radio sources lie in the northern hemisphere. The positions of magnetic field lines at $L = 6$ (L shell of Io) corresponding to the 10–40 MHz range of the electron gyrofrequency, are plotted using the O_4 model [Acuña and Ness, 1976]. A circle centered on the point of the Io flux tube for which the gyrofrequency equals 30 MHz is drawn in projection on the sky background. This gives a rough illustration of the angle between the magnetic field at the source and the direction of the Earth; the angle appears to be more acute for Io–A than for Io–B. This is consistent with our comparison of the relative ellipticities of Io–A and Io–B radiations. The thick line corresponds to the average direction that we have determined for the six Io–B events.

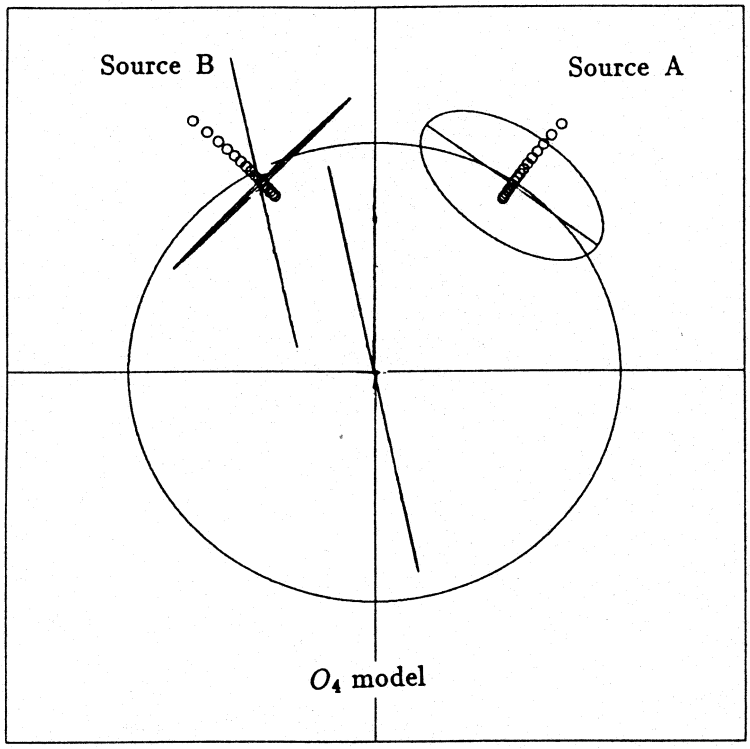

Figure 9: Representation of the positions of magnetic field lines that correspond to the 10–40 MHz range of electron gyrofrequency (circles) from the O_4 model. In each of the Io–A and Io–B cases, a circle perpendicular to the field line at the point where the electron gyrofrequency is 30 MHz, is drawn in projection on the sky. The thick line shows the orientation of polarization ellipse at Jupiter derived from the six Io–B events analysed in this paper.

The orientation of the polarization vector that we have found, seems to have no simple relation with the magnetic field geometry. There is no available theoretical description of the polarization of planetary auroral emissions. Moreover, the orientation of the polarization ellipse cannot be described by the simple geometrical model used to construct Figure 9. Aubier and Genova [1985], by studying the high frequency limit of DAM emissions observed by the Voyager spacecraft, found that the maximum observed emission frequency was not in agreement with the local gyrofrequency as deduced from the O_4 model. Our results cannot easily be interpreted in terms of the O_4 model. Dulk [1965, 1967], proposed that the Io–A and Io–B emissions result from the alignment of the observer with opposite sides of a single, hollow–cone emission beam. It would seem, therefore, that if the radiation propagates in the same hollow–cone, the Io–A and Io–B emission should exhibit comparable polarization but we find here that this is not the case. The difference is not likely due to terrestrial ionosphere, but must originate at Jupiter in the vicinity of the radio source.

6 Conclusion

For most accurate measurements done at three Io–B emissions, the polarization angle at Jupiter is found, on average, to be at position angle $+15°$ from the Jovian northern pole. We have shown that the linear approximation generally used to determine the angle of the polarization ellipse at Jupiter and the amount of rotation in the Earth's ionosphere is not valid. The quadratic approximation is better able to explain the observations because it includes a parameter which describes the curvature of the wave propagation. A comparison with the O_4 model shows that this value differs by more than 45 degrees

from the expected one. Unlike Io–B, Io–A events exhibit a random distribution, probably because the observable frequency range is smaller than that for Io–B, leading to a large uncertainty for the polarization angle. In addition, it is important to emphasize that Io–A emission is less elliptical than that of Io–B. It is possible that these differences may be due to the different emission geometries for the two sources, and may differ from event to event.

References

Acuña, M.H., N. F. Ness, The main magnetic field of Jupiter, *J. Geophys. Res.*, **81**, 2917, 1976.

Aubier, M.G., F. Genova, A catalogue of the high frequency limit of the Jovian decameter emission observed by Voyager, *Astron. Astrophys. Suppl. Ser.*, **61**, 341, 1985.

Boischot, A., C. Rosolen, M. G. Aubier, G. Daigne, F. Genova, Y. Leblanc, A. Lecacheux, J. de la Noë, B. Möller–Pedersen, A new high gain, broadband, steerable array to study Jovian decametric emissions, *Icarus*, **43**, 399, 1980.

Budden, K. G., The propagation of radio waves in the ionosphere (Cambridge Univ. Press), 1985.

Dulk, G. A., Io–related radio emission from Jupiter, *Ph. D. Thesis, University of Colorado, Boulder*, p. 226–284, 1965.

Dulk, G. A., Apparent change in the rotation rate of Jupiter, *Icarus*, **7**, 173, 1967.

Erickson, W. C., J. R. Fisher, A new wideband, fully steerable, decametric array at Clark Lake, *Radio Science*, **9**, 387, 1974.

Lecacheux, A., Spectral study of the polarization of the Jovian decametric radio, *Astron. Astrophys.*, **49**, 197, 1976.

Lecacheux, A., A. Boischot, M. Y. Boudjada, and G.A. Dulk, Spectra and complete polarisation state of two, Io-related, radio storms from Jupiter, *Astron. Astrophys.*, **251**, 339, 1991.

Parker, G. D., G. A. Dulk, J. W. Warwick, Faraday effect on Jupiter's radio bursts, *Astrophys. J.*, **157**, 439, 1969.

Phillips, J. A., T. C. Ferree, J. Wang, Earth-based observations of Faraday rotation in radio bursts from Jupiter, *J. Geophys. Res.*, **94**, 5457, 1989.

Riihima, J. J., Faraday rotation effects in spectral records of Jupiter's decametric radiation, *The Observatory*, **87**, 24, 1967.

Ross, W. J., Second–order effects in high–frequency transionospheric propagation, *J. Geophys. Res.*, **70**, 597, 1965.

Straka, R. M., C. L. Bennet, D. Gaunt, *Faraday rotation measurements of decameter wavelength radiation from the planet Jupiter in Electron Density Profiles in the Ionosphere and Exosphere*, edited by J. Frihagen, 1965.

Warwick, J. W., G. A. Dulk, Faraday rotation on decametric radio emission from Jupiter, *Science*, **145**, 380, 1964.